Recent history of sediment dynamics in Lake Toro and applicability of ^{210}Pb dating in a highly disturbed catchment in northern Japan

Young Sang Ahn[1,3*], Futoshi Nakamura[1], Kun Woo Chun[2]

[1] Department of Forest Science, Graduate School of Agriculture, Hokkaido University

[2] Division of Forest Resources, College of Forest and Environmental Sciences, Kangwon National University

[3] Division of Forest Restoration, Korea Forest Research Institute

Young Sang Ahn
Division of Forest Restoration, Korea Forest Research Institute, 57 Hoegi-Ro, Dongdaemun-Gu, Seoul, 130-712, Republic of Korea.
E-mail: ysahn@forest.go.kr

Futoshi Nakamura
Laboratory of Forest Ecosystem Management, Graduate School of Agriculture, Hokkaido University, Sapporo, Hokkaido 060-8589, Japan
E-mail: nakaf@for.agr.hokudai.ac.jp

Kun Woo Chun
Division of Forest Resources, College of Forest and Environmental Sciences, Kangwon National University, 192-1 Hyoja-dong, Chuncheon, Gangwondo 200-701, Republic of Korea.
E-mail: kwchun@kangwon.ac.kr

[*] Corresponding author
Young Sang Ahn
Division of Forest Restoration, Korea Forest Research Institute, 57 Hoegi-Ro, Dongdaemun-Gu, Seoul, 130-712, Republic of Korea.
Phone: +82-2-961-2644. Fax: +81-2-961-2649.
E-mail: ysahn@forest.go.kr

Abstract

Sediment dynamics for the last 300 years in Lake Toro and the applicability of ^{210}Pb dating (CIC and CRS models) are here evaluated. The lake sedimentation and sediment yield were determined by ^{137}Cs (1963) and two tephra layers (Ko-c2 in 1694 and Ta-a in 1739). The average sediment yields for initial development periods of catchments were 13.0–14.1 t km^{-2} yr^{-1} until 1963 and increased to 30.5 t km^{-2} yr^{-1} after 1963 because of the conversion of floodplain and upland forests to cultivated lands. In particular, the western zone of the lake near the conjunction with the Kushiro River had a high sedimentation rate, which is attributable to sediment inflow back from the Kushiro River during floods. The CIC model was not applicable because of fluctuations in the ^{210}Pb profiles since 1963. The CRS model agrees with the ^{137}Cs dating in all sites except for one site close to the Kushiro River inflow. ^{210}Pb dating may contain considerable errors where the ^{210}Pb concentration profile and flux is perturbed by floodwater from the Kushiro River, which contains low levels of ^{210}Pb.

Keywords: Lake sedimentation; Sediment yield; ^{210}Pb dating; ^{137}Cs dating; Kushiro Mire

1. Introduction

Human activities, such as deforestation, agricultural development, and stream channelization, have increased sediment production (Davis, 1976; Nakamura et al., 1997; Walling et al., 2003). The fine sediments eventually accumulate in lakes and wetlands (Nakamura et al., 1997), and sediment cores there reflect historical erosion rates in the catchments. Lakes have gradually become shallow due to a rapid accumulation of sediment delivered from the disturbed catchments (Ritchie et al., 1983:

Ahn et al., 2006; Singh et al., 2008). Thus, the historical record of lake sedimentation is important for understanding the lake environment with respect to land use in the catchment.

Lake sediment cores are used for reconstructing sedimentation histories. Accurate sediment chronologies are crucial for interpreting historical sediment dynamics. Volcanic tephra dating is popular, but it is limited to landscapes that have preserved ash layers (Ahn et al., 2006). Other radiometric dating using ^{137}Cs and ^{210}Pb profiles was widely used to examine the last 100–150 years in lake and reservoir environments (Foster et al., 1985, 1986). Two models, commonly referred to as the CIC (constant initial ^{210}Pb concentration) and CRS (constant rate of ^{210}Pb supply) models (Appleby and Oldfield, 1978), have been proposed to estimate dates using ^{210}Pb. The dating by the CIC model is accurate in stable environments with uniform sediment accumulation rates. The CRS model also gives good results at many sites with non-uniform accumulation. However, the ^{210}Pb-based chronology (CIC and CRS models) may contain errors when a large amount of sediment adsorbing ^{210}Pb is delivered from the above catchment, because it violates the assumptions of constant concentration and flux of ^{210}Pb (Marques Jr. et al., 2006). Thus, it is important to examine the applicability of ^{210}Pb dating to lake sediment using independent chronological evidence wherever possible. The best means for validating dates for the last 40 years is through records of an artificial radionuclide, ^{137}Cs (Appleby, 2001).

Many rivers and streams in Japan are channelized, and the floodplains and gentle hillslopes have been used for cattle grazing and crop cultivation since the 1960s. The Kushiro Mire, the largest wetlands complex in Japan, is home to a diversity of wetland wildlife. However, excessive production and transport of suspended sediment and

nutrients are evident in association with deforestation, pasture development, and stream channelization (Nakamura et al., 2002, 2004). There are three lakes on the eastern margin of the mire, and recently they have suffered from accelerated sedimentation and a decline in water quality because of the influx of nutrient-rich, turbid water (Takamura et al., 2003; Hokkaido Institute of Environmental Sciences, 2005; Ahn et al., 2008). In particular, Lake Toro, the largest lake, has suffered degradation and eutrophication from intensive pasture development in the catchment. Recent studies have indicated that water quality and aquatic plant species in Lake Toro are being rapidly degraded (Takamura et al., 2003). The Hokkaido Institute of Environmental Sciences (2005) also reported deterioration of the spawning habitat of Japanese smelt (*Hypomesus nipponensis*) due to accumulation of fine sediment. However, there are no studies examining the recent history of sediment accumulations with reference to land use in the Lake Toro catchment.

This study aimed to elucidate the recent history of lake sedimentation using ^{137}Cs, ^{210}Pb and tephrochronology. The dating results by ^{137}Cs and ^{210}Pb were cross-checked to examine the applicability of ^{210}Pb dating (CIC and CRS models) in the Lake Toro catchment, which has been highly disturbed over the past 50 years. The present study focused on sediment dynamics over the last 300 years using ^{137}Cs and tephrochronology as chronological markers. In particular, this study examined the relationship between the spatial variation of sedimentation rates and the sediment yields from the catchments together with changes in land use.

2. The study site

Lake Toro is located on the east margin of the Kushiro Mire in eastern Hokkaido, in northern Japan. The lake is located in the Pacific coast climatic zone. The annual mean

air temperature at the Kushiro Meteorological Observatory is 6.0 °C measured from 1971 to 2006 (Japan Meteorological Agency, 2007). The annual mean precipitation is 1037 mm, with a range of 705–1378 mm. The Kushiro Mire (194 km^2) drains into the Kushiro River (2510 km^2) (Fig. 1). Lake Toro has an area of 6.3 km^2, drains a catchment area of 133.2 km^2 and eventually flows into the Kushiro River (Fig. 1).

The sea level gradually rose along the coastlines of Japanese archipelago since the Last Glacial Maximum, and it reached a peak level about 6000 years ago. Thereafter the sea level descended three to five meters. The elevations of the eastern Pacific coast of Hokkaido become higher than modern mean tidal level (MTL) 3000 years ago (Sawai, 2002; Sawai et al., 2002). As a result, inland areas that were lower than the MTL became lakes and wetlands gradually. Lake Toro was formed 3000 years ago as the sea level descended.

The Arekinai and Omoshironbetsu Streams and other small tributaries flow into Lake Toro (Fig. 1). The water levels of Lake Toro and the Kushiro River are almost equal at base flow conditions. When the water level of the Kushiro River rises, water flows back into the lake (Hokkaido Institute of Environmental Sciences, 2005; Ahn et al., 2008). The average water depth in the lake is 6.0 m (Table 1), and the maximum water depth is 7.3 m. Lake Toro is surrounded by hills to an elevation of 100 m. The humic layer has crumbly soil. The subsurface soil texture is a silty loam and is thicker on the terraces than on the hillside slopes. The bedrock consists of tertiary gravel and sand stones. The northern slope of the Lake Toro catchment is a steep forest. The southern and eastern uplands gradually descend to the lake, and areas of the lower elevations are intensively cultivated for livestock (Fig. 1). The forest cover is comprised of planted forests (*Larix leptolepis*) and indigenous forests (mainly *Quercus crispula*).

Prior to modern Japanese settlement in the Lake Toro catchment, Ainu (indigenous people) had been using the area for hunting and fishing as well as for crop cultivation and timber harvesting. The catchment was the most popular Ainu settlement site in the Kushiro Mire because of natural resources such as water, forests, and fertile soil. As the Japanese settlement began in the 1880s, indigenous forest was partly cleared for charcoal production (Kumagai et al., 2008). Group settlement in the Lake Toro catchment occurred after road construction in 1939, and the dairy industry was established (Shibecha cyoushihensaniinkai, 2002). In the 1960s, pastures for milk production expanded. Agricultural drainage construction and further land consolidation projects were undertaken in the Arekinai Stream catchment from 1972 to 1986 (Shibecha cyoushihensaniinkai, 2006). Since then, the dairy industry has continued to grow, especially in the Arekinai Stream catchment (Fig. 1). The Arekinai Stream catchment has been gradually converted into farmlands through the introduction of buried and open ditch drainage systems. Although reforestation with *L. leptolepis* aimed to recover the forest resources, the demand for lumber remains.

3. Methods

3.1 Sediment sampling

To evaluate sedimentation rates in Lake Toro, sediment cores were collected from 28 points in June 2006 (Fig. 1). Sampling points were classified according to their geographical setting: seven sampling points in the eastern zone where the Arekinai and Omonshironbetsu Streams flow into the lake (E1–E7), five sampling points in the western zone where the lake water flows into the Kushiro River under low flow conditions and floodwater of the Kushiro River flows back into the lake during floods

(W1–W5), and sixteen sampling points in the middle where small tributaries enter (M1–M16).

Core samples were extracted by a 7.2 cm diameter polyvinyl chloride tube. All core samples were dissected into 1 cm-thick slices and were preserved in a sealed container at –10 °C. Dry bulk density was calculated after drying for 24 h at 105 °C.

3.2 Dry bulk density of the lake sediments

The most distinctive and widespread tephras over the study areas were Komagatake-c2 tephra (1694 AD) and Tarumae-a tephra (1739 AD). Ahn et al. (2006) identified two tephra layers from Lake Takkobu in the Kushiro Mire. The dry bulk density of the tephra sediment in Lake Takkobu was high compared with that of the fluvial sediment transported from the catchment (Ahn et al., 2006). To remove the effects of possible sediment compaction on the dry bulk density distributions during sampling, cumulative dry mass depth was used.

3.3 ^{137}Cs and ^{210}Pb dating

^{137}Cs from atomic bomb testing first entered the environment in the early 1950s and peaked in 1963, which provides easily identifiable chronological markers in lake sediment (He et al., 1996; Appleby, 2001; Walling et al., 2003). Because ^{137}Cs is strongly adsorbed into fine sediment particles, its redistribution occurs in association with sedimentary particles. In the Kushiro Mire, a 1963 ^{137}Cs peak is readily identifiable and has been used as a chronological marker (Ahn et al., 2006; Mizugaki et al., 2006).

^{210}Pb, a naturally occurring radionuclide (half-life 22.3 years), is a product of the ^{238}U decay series, derived via a series of other short-lived radionuclides from the decay of gaseous ^{222}Rn (half-life 3.8 days), the daughter of ^{226}Ra (half-life 1622 years). The

^{210}Pb content of soils and rocks produced by the in situ decay of ^{226}Ra is termed 'supported ^{210}Pb' because it is in equilibrium with its parent. However, upward diffusion of a small portion of the ^{222}Rn produced naturally in soils and rocks releases ^{222}Rn to the atmosphere, and the subsequent fallout of ^{210}Pb is incorporated into surface soils and sediments, which are not in equilibrium with ^{226}Ra. Such ^{210}Pb fallout is commonly termed 'unsupported ^{210}Pb.' Because of its natural origin, the deposition of ^{210}Pb has been, unlike that of ^{137}Cs, essentially constant through time (Nozaki et al., 1978).

The unsupported ^{210}Pb in each sediment layer declines in accordance with radioactive decay. The sedimentation rates can be estimated assuming that the flux of unsupported ^{210}Pb into the lake sediment is constant (Appleby et al., 1979). As unsupported ^{210}Pb in deposited sediment decays according to its half-life, the unsupported ^{210}Pb profile in the sediment decreases exponentially with constant sedimentation. The model to estimate sedimentation rate with a constant input of unsupported ^{210}Pb is the CIC (Constant Initial Concentration) model. Assuming constant unsupported ^{210}Pb flux, a sedimentation rate at a given depth can be estimated by attributing a decrease in unsupported ^{210}Pb in the depth profile to radioisotope decay (Appleby and Oldfield, 1978; 1983). This approach is the CRS (Constant Rate of Supply) model.

To measure ^{137}Cs and unsupported ^{210}Pb activity, gamma spectrometry was employed at the Central Institute of Isotope Science, Hokkaido University. The ^{137}Cs activity was measured using P-type HPGe detectors (Ortec and PGT, USA), and the unsupported ^{210}Pb activity was analyzed using an N-type GMX HPGe coaxial detector (Ortec, USA), both coupled with a multichannel analyzer (SEIKO EG&G MCA7700,

Japan). In gamma ray spectrometry for ^{210}Pb dating, the unsupported ^{210}Pb activities were determined from the difference between total and supported ^{210}Pb activities. Assuming equilibrium between the ^{226}Ra and ^{222}Rn in the soil samples, the supported ^{210}Pb activities can be calculated from the activity of its short-lived daughter product, ^{214}Pb (half life of 27 min), which is derived from ^{222}Rn in the ^{238}U decay series (Joshi, 1987; Murray et al., 1987).

The ^{137}Cs and unsupported ^{210}Pb contents of the cores were measured at 2 cm intervals. The sediment samples were dried for 24 hours at 105 °C. All the samples were gently ground, passed through a 2 mm-mesh sieve, and thoroughly mixed before the gamma assay. ^{137}Cs profiles were constructed for 28 sediment cores. ^{210}Pb samples in the tubes for five cores (Sites E4, M7, M10, M16, and W2) were sealed and left for 21 days before analysis to allow for equilibrium between ^{226}Ra and ^{222}Rn. For ^{137}Cs and ^{210}Pb analyses, the gamma activities of each sediment sample were measured for 36,000 seconds. Using HPGe detectors, gamma activity was 661.6 keV for ^{137}Cs, 46.5 keV for total ^{210}Pb, and 352.0 keV for ^{214}Pb. Two of ^{214}Pb γ-emissions easily detected by a HPGe detector are at 295.2 keV (18.9 %) and 352.0 keV (36.7 %). Because of a relatively higher branching ratio for the 352.0 keV emission, this photopeak provides better sensitivity (Joshi, 1987). Therefore, in our measurements we employ only the 352.0 keV photopeak for deriving concentrations of ^{226}Ra.

3.4 Estimation of sediment yield

Total sediment mass in the lake was calculated to determine the temporal change in sediment yield in the Lake Toro catchment. The average sedimentation rates (g cm^{-2} yr^{-1}) were calculated using ^{137}Cs measurements and tephrochronology as follows:

$SR_i = D_i / T_i$

where SR_i is the average sedimentation rate (g cm^{-2} yr^{-1}), D_i is the cumulative dry mass depth between markers (g cm^{-2}), and T_i is the chronological time interval (years). The average sedimentation rates were plotted at each coring location and contoured using ERDAS IMAGINE. The total sediment mass was estimated by multiplying the average sedimentation rates in each zone by its area and by planimetric calculations based on the contours.

The sediment yield was estimated by dividing the total sediment mass in the lake by the area of the catchment draining into the lake. This method assumes that all the sediment from the contributing catchments is deposited in the lake and is not transported out of the lake. This assumption is not correct because some sediment is exported into the Kushiro River. The Brune (1953) median trap efficiency curve (the percentage of sediment input that is retained in the reservoir) was used to adjust the sediment yields. In order to estimate the ratio of the lake capacity to the average annual inflow of water (C/I ratio), average annual inflows of water were obtained from the Hokkaido Institute of Environmental Sciences (Table 1). The trap efficiency of the lake depends upon C/I ratio, and lake capacity is significantly influenced by sediment accumulation. We changed the lake capacity according to the sediment accumulation in each period, although the average annual inflow of water was assumed to be constant throughout the periods. As a result, the trap efficiency was estimated at each period.

4. Results

4.1 The distribution of dry bulk density of the lake sediments

The dry bulk density peaks are different at depths where volcanic tephra sediment is present, except for Points M5, W4, and W5 (Fig. 2). The volcanic tephra layer shows a

unique white-gray color unlike the lake sediment. The sediment above the volcanic tephra layer in all profiles contained a small amount of tephra sediment that may have been reworked by fluvial transport. The deepest volcanic tephra layers of Ta-a (1739) and Ko-c2 (1694) were found at Point E1 located near the inflow of the Arekinai Stream at depths of 28.1–29.4 g cm^{-2} and 31.8–33.3 g cm^{-2}, respectively (Table 2). In contrast, the shallowest tephra layer was found at Point M5 in the middle zone, having only one tephra layer with a pronounced dry bulk density peak at a depth of 4.9–7.1 g cm^{-2}. At Points W4 and W5 near the inflow of the Kushiro River, however, tephra layers were not detected, despite core sediments obtained to depths of 42.1 g cm^{-2} and 49.4 g cm^{-2}, respectively.

4.2 ^{137}Cs and ^{210}Pb dating

All profiles had a single peak of ^{137}Cs concentrations. The ^{137}Cs concentration gradually decreased from the peak to the surface layer of the profile, whereas it dropped sharply below the peak (Fig. 3). The highest peak concentration in a profile was considered to be the sediment stratum of the 1963 fallout maximum (Ritchie et al., 1983; He et al., 1996; Ahn et al., 2006; Mizugaki et al., 2006). The shallowest peak among all the samples was at a depth of 2.1–2.4 g cm^{-2} at Point M4, which was located in the middle zone (Fig. 3). Other sites in the middle zone, such as Points M8, M11, and M12, had a peak concentration at a depth of 2.3–2.6 g cm^{-2} (Table 2). The sampling sites in the middle zone had a peak concentration in shallow depths. In contrast, Point W4, located close to the confluence of the Kushiro River, had a peak concentration at its deepest layer of 15.8–16.4 g cm^{-2}, which was seven times deeper than M4.

^{137}Cs and unsupported ^{210}Pb activities were analyzed for the cores E4, M7, M10, M16, and W2 (Fig. 4). The unsupported ^{210}Pb depth distribution for these cores revealed

a nonexponential decrease with increasing depth and exhibited several fluctuations. In particular, a significant reduction of the unsupported ^{210}Pb activity was shown at 1.3–2.4 g cm^{-2} in Point E4, at 1.1–2.6 g cm^{-2} in Point M7, at 1.0–1.6 g cm^{-2} in Point M16, and above 6.7 g cm^{-2} in Point W2. The ^{210}Pb dating was calculated using the CRS model because the CIC model does not fit the non-monotonic unsupported ^{210}Pb profiles. To examine the applicability of the CRS model to evaluation of lake sedimentation rates in a highly disturbed catchment, the depths of sediment deposited in 1963 as determined by the CRS model were cross-checked against the date obtained by the ^{137}Cs dating (Fig. 5). The age calculated using the CRS model in Lake Toro profiles was in good agreement with ^{137}Cs, except at Point W2, which is close to the inflow of the Kushiro River (Fig. 5).

4.3 Lake sedimentation

The ^{137}Cs peak and the two tephra layers were identified in all profiles, except at Points M5, W4, and W5 (Table 2). With regard to the Point M5 core, only one tephra layer was identified, suggesting that the two tephra layers had merged because of a low sedimentation rate. The absence of tephra in Points W4 and W5 samples means that Ta-a tephra (1739) may exist below the sampling depths. For points where no Ta-a tephra was found in the profile, the sedimentation rates for 1739–1963 were calculated as a minimum value by assuming the maximum sampling depth as the 1739 layer (Table 2). The sedimentation rates between 1694–1739 could not be estimated. The average sedimentation rates were compared over the three periods (1694–1739, 1739–1963, and 1963–2006) of the last 300 years and among locations in the lake (Fig. 6). The sedimentation rates between 1694–1739 were relatively low, and sediment transported from the catchment evenly accumulated over the lake bottom, except at the inflows of

the Arekinai and Omoshironbetsu Streams. In contrast, sediment delivered in 1739–1963 was concentrated at the inflows of the Kushiro River and the Arekinai Stream but was distributed thinly (less than 0.02 g cm^{-2} yr^{-1}) over the lake. The sedimentation rate after 1963 greatly increased. In particular, the sedimentation rate at inflows from the Kushiro River exhibited high sedimentation rates in this period, and sediment delivered to the lake was broadly distributed over the lake bottom (Fig. 6).

4.4 Sediment yield

The total sediment mass in the lake was 1787 t yr^{-1} in 1694–1739 and 1640 t yr^{-1} in 1739–1963. The total sediment mass after 1963 increased to 3855 t yr^{-1}. Compared with the sediment mass of 1714 t yr^{-1} prior to 1963, sediment production and delivery accelerated after 1963.

The sediment trap efficiency over the three periods (1694–1739, 1739–1963, and 1963–2006) were 95.2, 94.8, and 94.6 %, respectively. The sediment yields of the lake catchment were 14.1 and 13.0 t km^{-2} yr^{-1} for 1694–1739 and 1739–1963, respectively, and 30.5 t km^{-2} yr^{-1} for 1963–2006 (Fig. 7). The average sediment yield in the Lake Toro catchment after 1963 was more than twice that before 1963.

5. Discussion

5.1 The applicability of ^{210}Pb dating

The CIC model was not applicable to lake sediment because of the non-monotonic trend of unsupported ^{210}Pb (Fig. 4). However, the dates by CRS model at all points are in good agreement with the dates by ^{137}Cs. The differences between the two dating methods are within 10 years, except for Point W2 (Fig. 5). The basic assumption of the CRS model is that the supply rate of unsupported ^{210}Pb from the atmosphere is constant

(Appleby and Oldfield, 1983; Appleby, 2001). Unsupported ^{210}Pb is removed from the atmosphere by precipitation, quickly adsorbed onto suspended sediments, and deposited in lakes and oceans. The unsupported ^{210}Pb concentration in sediment layers will be inverse to the sedimentation rate. The concentration of unsupported ^{210}Pb above the ^{137}Cs peak (1963) in Lake Toro exhibited a considerable fluctuation (Fig. 4). The Lake Toro catchments have seen forest converted into farmland since the 1960s, which has increased sediment yield and subsequent lake sedimentation (Figs 6 and 7). The elevated and variable sediment flux from the catchment may dilute and disturb the unsupported ^{210}Pb concentration in Lake Toro, which causes fluctuations in the unsupported ^{210}Pb concentration of the sediment cores.

At Point W2 near the inflow of the Kushiro River, the concentration of unsupported ^{210}Pb above the ^{137}Cs peak (1963) decreased abruptly (Fig. 4). In addition, the age calculated using the CRS model at Point W2 was not in agreement with ^{137}Cs (Fig. 5). This can be attributed to the sharp increase in the sedimentation rate in the period 1963–2006 at Point W2 (Fig. 6). Lake Toro drains into the Kushiro River at base flow conditions but has suffered from floodwater inflows from the Kushiro River (Hokkaido Institute of Environmental Sciences, 2005; Ahn et al., 2008). The Kushiro River catchment has been intensively developed since the 1960s through timber harvesting, pasture development, and river channelization. In association with these activities, floodwater containing large amounts of fine sediment and nutrients has been introduced into the Kushiro River (Nakamura et al., 1997, 2004; Ahn et al., 2008). A large sediment influx containing a low level of the unsupported ^{210}Pb concentration from the Kushiro River could lower the overall unsupported ^{210}Pb concentration at Point W2. Moreover, the repeated inflows of floodwater from the Kushiro River may perturb the

profile of the unsupported ^{210}Pb concentration and may cause errors in the CRS model (Fig. 5). Thus, the CRS model is not applicable to sites where the episodic and infrequent sediment flux occurs with complex hydrology in a catchment.

5.2 Recent history of sediment dynamics

Many Ainu, indigenous people, resided in the Lake Toro catchment. They mainly used the area for crop cultivation and timber harvesting, but their exploitation of natural resources was very limited. Japanese settlement around the lake catchment started in the 1880s, and the forest was partly harvested for charcoal production (Shibecha cyoushihensaniinkai, 2002; Kumagai et al., 2008). The road was constructed in 1939 to promote milk production and group settlement (Shibecha cyoushihensaniinkai, 2002). However, Japanese settlement until the 1950s was not extensive because they did not want to live with indigenous people (personal communication with local residents). Farmland development has expanded in the floodplain and hillslope areas at low and intermediate elevations since Japanese economic growth in the 1950s. Land consolidation projects in the 1960s promoted the combination of small farms and the introduction of agricultural machinery (Shibecha cyoushihensaniinkai, 2006). Development of the Kushiro River watershed began in 1880s with Japanese group settlement and river channel excavation (Koaze et al., 2003). In the 1940s, floodplain wetlands in the Kushiro River watershed were developed into cattle farms, and since the 1960s, land consolidation and the introduction of agricultural machinery have been promoted (Nakamura et al., 2004).

The sediment yields for 1694–1739 reflect semi-natural conditions managed by indigenous people, whereas those for 1739–1963 reflect the partially deforested condition associated with charcoal production, road construction, and crop cultivation

by Japanese settlers. The yield from 1963 to 2006 indicates the over-exploited clearance of the native forests for timber production and the use of modern agricultural machinery. The average sediment yield in the Lake Toro catchment after 1963 (30.5 t km^{-2} yr^{-1}) was more than twice that before 1963 (14.1 and 13.0 t km^{-2} yr^{-1}) (Fig. 7). The clearance of native mature forests and large-scale farming in the Lake Toro catchment after 1963 accelerated sediment yields, which resulted in a large amount of sediment delivery into the lake.

The sedimentation in Lake Toro varied greatly with historical land use and hydrogeomorphic conditions (Fig. 6). The sedimentation rates in 1694–1739 were low and showed few differences among the sites, except at the inflow areas of Arekinai and Omoshironbetsu Streams. This spatial pattern reflects semi-natural (reference) conditions with limited activities by indigenous people. Although average sedimentation rates were still low in 1739–1963 (Fig. 7), the spatial pattern of sediment accumulation had started to change, as indicated by an elevated sedimentation at two major inflows from Kushiro River and Arekinai Stream. These concentrated accumulations of sediment may reflect land use changes in this period. The land use development in the Kushiro River watershed was initiated from early periods (from 1880 to the 1890s), and floodplains were cultivated for cattle farming in the 1940s. Floodplain cultivation for food production began in the Arekinai Stream watershed in the 1950s. These initial developments may have delivered pulses of sediment into the lake and deposited them at the mouths of the two major rivers.

The elevated sedimentation rates at inflows from the Kushiro River and Arekinai Stream in 1739–1963 continued in 1963–2006, although their rates were further accelerated, and sediment was delivered not only to the eastern and western zones but

also to the middle zone (Fig. 6). This suggests that the sediment produced from the contributing catchments accumulates mostly near the mouth of stream channels entering the lake and decreases toward the center (Ahn et al., 2006). The lake sedimentation after 1963 increased greatly (Fig. 6). Point W4 in the period 1963–2006 had the highest sedimentation rate among all points because of sediment influx from the Kushiro River into the lake during high flow discharges (Fig. 6). Since the 1960s, cultivation has been promoted in the Kushiro River catchment, which has produced a high sediment load in the Kushiro River (Ahn et al., 2008). Also, Points E2 and E5, located near the mouth of the Arekinai Stream, exhibited high sedimentation rates because of rapid expansion of farmlands in floodplains and adjacent hill slopes in the Arekinai Stream catchment (Fig. 1).

Sediment dynamics of Lake Toro are complex. The lake has suffered from sediment loads from its tributaries (especially from the Arekinai Stream) and also from the Kushiro River. However, the sedimentation rates in 1963–2006 at Points E1 and W5 decreased in comparison with those before 1963, although other sites exhibited significant increases (Fig. 6). As a lake becomes shallow, the sediment trap efficiency can be reduced (Lajczak, 1996). These decreases in the sedimentation rates may be explained by steepening of the lake bottom slope with sedimentation and the resultant reduction of sediment retention capacity.

Acknowledgements

The authors are grateful to Mr. Yoshifusa Suzuki of the Ocean Research and Systems Co. Ltd., Japan for field assistance and to Mr. Hidetoshi Mikami of the Hokkaido Institute of Environmental Sciences for providing the average annual inflow of water data. The Central Institute of Isotope Science, Hokkaido University, Japan assisted with

analyses. We also wish to thank the president of the Toro Fishing Cooperative Association, Yoshinori Tosa, for his advice throughout this study. This research was supported by Grants-in-Aid for Scientific Research (18-06208, 18201008, 19208013) from the Ministry of Education, Japan.

References

Ahn, Y.S., Mizugaki, S., Nakamura, F., Nakamura, Y., 2006. Historical change in lake sedimentation in Lake Takkobu, Kushiro Mire, northern Japan over the last 300 years. Geomorphology 78, 321–334.

Ahn, Y.S., Nakamura, F., Mizugaki, S., 2008. Hydrology, suspended sediment dynamics and nutrient loading in Lake Takkobu, a degrading lake ecosystem in Kushiro Mire, northern Japan. Environmental Monitoring and Assessment 145, 267–281.

Appleby, P.G., 2001. Chronostratigraphic techniques in recent sediments. In: Last, W.M., Smol, J.P. (Eds.), Tracking Environmental Change using Lake Sediments (Vol. 1): Basin Analysis, Coring, and Chronological Techniques. Kluwer Academic Publishers, Dordrecht, The Netherlands, pp. 171–203.

Appleby, P.G., Oldfield, F., 1978. The calculation of ^{210}Pb dates assuming a constant rate of supply of unsupported ^{210}Pb to the sediment. Catena 5, 1–8.

Appleby, P.G., Oldfield, F., 1983. The assessment of ^{210}Pb data from sites varying sediment accumulation rates. Hydrobiologia 103, 29–35.

Appleby, P.G., Oldfield, F., Thompson, R., Huttenen, P., Tolonen, K., 1979. ^{210}Pb dating of annually laminated lake sediments from Finland. Nature 280, 53–55.

Brune, G.M., 1953. Trap efficiency of reservoirs. Transactions of the American Geophysical Union 34, 407–418.

Davis M.B., 1976. Erosion rates and land-use history in southern Michigan. Environmental Conservation 3, 139–148.

Foster, I.D.L., Dearing, J.A., Appleby, P.G., 1986. Historical tends in catchment sediment yield: a case study in reconstruction from lake-sediment records in Warwickshire, UK. Hydrological Sciences 31, 427–443.

Foster, I.D.L., Dearing, J.A., Simpson, A., Carter, A.D., Appleby, P.G., 1985. Lake catchment based studies of erosion and denudation in the Merevale catchment, Warwickshire, U.K. Earth Surface Processes and Landforms 10,45–68.

He, Q., Walling, D.E., Owens, P.N., 1996. Interpreting the ^{137}Cs profiles observed in several small lakes and reservoirs in southern England. Chemical Geology 129, 115–131.

Hokkaido Institute of Environmental Sciences, 2005. Lakes and Marshes in Hokkaido (Revised edition). Hokkaido Institute of Environmental Sciences, Sapporo. (in Japanese)

Japan Meteorological Agency, 2007. http://www.jma.go.jp/jma/index.html (in Japanese).

Joshi, S.R., 1987. Nondestructive determination of lead-210 and radium-226 in sediments by direct photon analysis. Journal of Radioanalytical and Nuclear Chemistry 116, 169–182.

Koaze, T, Nogami, M., Ono, Y., Hirakawa, K., 2003. Regional geomorphology of the Japanese Islands. Vol. 2. Geomorphology of Hokkaido. University of Tokyo Press, Tokyo. (in Japanese)

Kumagai, Y., Ahn, Y.S., Nakamura, F., 2008. Recent human impact on vegetation in Takkobu, northern Japan, reconstructed from fossil pollen in lake sediments. Journal of Forest Research 13, 223–232.

Lajczak, A., 1996. Modelling the long-term course of non-flushed reservoir sedimentation and estimating the life of dams. Earth Surface Processes and Landforms 21, 1091–1107.

Marques Jr., A.N., Monna, F., Da Silva Filho, E.V., Fernex, F.E., Fernando Lamego Simões Filho, F., 2006. Apparent discrepancy in contamination history of a sub-tropical estuary evaluated through ^{210}Pb profile and chronostratigraphical markers. Marine Pollution Bulletin 52, 532–539.

Mizugaki, S., Nakamuara, F., Araya, T., 2006. Using dendrogeomorphology and ^{137}Cs and ^{210}Pb radiochronology to estimate recent changes in sedimentation rates in Kushiro Mire, Northern Japan, resulting from land use change and river channelization. Catena 68, 25–40.

Murray, A.S., Marten, R., Johnston, A., Martin, P., 1987. Analysis for naturally occurring radionuclides at environmental concentrations by gamma spectrometry. Journal of Radioanalytical and Nuclear Chemistry 115, 263–288.

Nakamura, F., Kameyama, S., Mizugaki, S., 2004. Rapid shrinkage of Kushiro Mire, the largest mire in Japan, due to increased sedimentation associated with land-use development in the catchment. Catena 55, 213–229.

Nakamura, F., Mieko, J., Kameyama, S., Mizugaki, S., 2002. Changes in riparian forest in the Kushiro Mire, Japan, associated with stream channelization. River Research and Applications 18, 65–79.

Nakamura, F., Sudo, T., Kameyama, S., Mieko, J., 1997. Influences of channelization on discharge of suspended sediment and wetland vegetation in Kushiro Marsh, northern Japan. Geomorphology 18, 279–289.

Nozaki Y., DeMaster, D.J., Lewis, D.M., Turekian, K.K., 1978. Atmospheric ^{210}Pb fluxes determined from soil profiles. Journal of Geophysical Research 83, 4047–4051.

Ritchie, J.C., Cooper, C.M., McHenry, J.R., Schiebe, F.R., 1983. Sediment accumulation in Lake Chicot, Arkansas. Environmental Geology 5, 79–82.

Sawai, Y., 2002. Evidence for 17th-century tsunamis generated on the Kuril-Kamchatka subduction zone, Lake Tokotan, Hokkaido, Japan. Journal of Asian Earth Sciences 20, 903–911.

Sawai, Y., Nasu, H., Yasuda, Y., 2002. Fluctuations in relative sea-level during the past 3000 yr in the Onnetoh estuary, Hokkaido, northern Japan. Journal of Quaternary Science 17(5–6), 607–622.

Shibecha cyoushihensaniinkai, 2002. Shibechacyoushi: Tsuushihen Dai2Ken. Gyousei co., Kushiro. (in Japanese)

Shibecha cyoushihensaniinkai, 2006. Shibechacyoushi: Tsuushihen Dai3Ken. Gyousei co., Kushiro. (in Japanese)

Singh, S., Thakural, L.N., Kumar, B., 2008. Estimation of sediment rates and life of Sagar Lake using radiometric dating techniques. Water Resources Management 22, 443–455.

Takamura, N., Kadono, Y., Fukushima, M., Nakagawa, M., Kim, B.H.O., 2003. Effects of aquatic macrophytes on water quality and phytoplankton communities in shallow lakes. Ecological Research 18, 381–395.

Walling, D.E., Owens, P.N., Foster, I.D.L., Lees, J.A., 2003. Changes in the fine sediment dynamics of the Ouse and Tweed basins in the UK over the last 100–150 years. Hydrological Processes 17, 3245–3269.

Figure legends

Fig. 1. Location of Lake Toro, the lake coring sites, and land use development in the surrounding catchments.

Fig. 2. The dry bulk density distribution of the sediment cores. The arrow denotes a tephra layer.

Fig. 3. The profiles of ^{137}Cs activity in the lake sediment. An asterisk indicates that the^{137}Cs activities are under the detection limit.

Fig. 4. The profiles of ^{137}Cs and unsupported ^{210}Pb activities at Points E4, M7, M10, M16, and W2. An asterisk indicates that the^{137}Cs and unsupported ^{210}Pb concentrations are under the diction limit.

Fig. 5. Dates in the lake cores calculated using CRS model ^{210}Pb together with date determined from ^{137}Cs stratigraphy.

Fig. 6. Patterns of sedimentation in Lake Toro for three periods.

Fig. 7. The average sediment yields reconstructed over the last 300 years.

Table captions

Table 1

Site characteristics of Lake Toro and its catchments

Catchment area (km^2)	133.2
- Arekinai Stream	- 83.3
- Omoshironbetsu Stream	- 20.5
- Barumai Stream	- 6.7
- Henekorobetsu Stream	- 5.7
- Onnebetsu Stream	- 3.0
- Other small tributaries	- 14.0
Agricultural land use (km^2)	58.8
A percentage of agricultural land area in the catchment area (%)	44.1
Lake area (km^2)	6.3
Average water depth (m)	6.0
Water volume (m^3)	32.0×10^6
Average annual inflow (m^3)	72.6×10^6

Table 2

The cumulative dry mass depth of the ^{137}Cs peak and tephra

Core point		^{137}Cs (g cm^{-2})	Tephra (g cm^{-2})	
		^{137}Cs peak	Ta-a	Ko-c2
Eastern zone	E1	2.9– 3.6	28.1–29.4	31.8–33.3
	E2	4.9– 5.4	15.4–17.5	21.6–23.4
	E3	2.7– 3.0	6.7– 8.6	9.9–11.2
	E4	3.6– 3.9	8.0–10.1	12.0–14.3
	E5	5.6– 6.0	11.0–12.4	14.0–14.8
	E6	2.9– 3.1	7.4– 9.7	11.6–13.2
	E7	3.1– 3.4	7.2– 7.8	8.8– 9.7
Middle zone	M1	3.0– 3.3	7.3– 9.0	10.4–11.9
	M2	3.1– 3.4	6.2– 8.0	9.5–10.9
	M3	2.5– 2.7	5.4– 7.6	8.4– 9.4
	M4	2.1– 2.4	6.1– 8.8	10.5–11.6
	M5	2.4– 2.7	4.9 – 7.1	
	M6	2.5– 2.9	5.4– 6.7	7.7– 8.2
	M7	2.6– 2.8	5.6– 7.4	8.5– 9.5
	M8	2.3– 2.6	6.5– 8.4	9.3–10.5
	M9	2.7– 2.9	6.1– 7.1	8.3–10.2
	M10	2.6– 2.8	6.4– 7.6	9.3– 9.9
	M11	2.3– 2.6	6.1– 8.2	9.1–10.5
	M12	2.4– 2.6	5.7– 6.6	7.4– 9.5
	M13	2.8– 3.0	6.5– 8.4	9.0–10.5
	M14	2.5– 2.8	4.8– 6.3	7.4– 9.4
	M15	3.7– 3.9	7.4– 9.7	11.7–12.6
	M16	2.7– 3.1	5.7– 7.8	9.6–10.4
Western zone	W1	3.2– 3.6	8.9–11.2	12.8–13.9
	W2	6.3– 6.7	15.6–18.2	20.4–21.8
	W3	5.2– 5.6	17.2–20.2	21.5–23.4
	W4	15.8–16.4	41.4–42.1*	–
	W5	4.3– 4.6	48.9–49.4*	–

An asterisk indicates that the maximum sampling depth is considered as a tephra layer

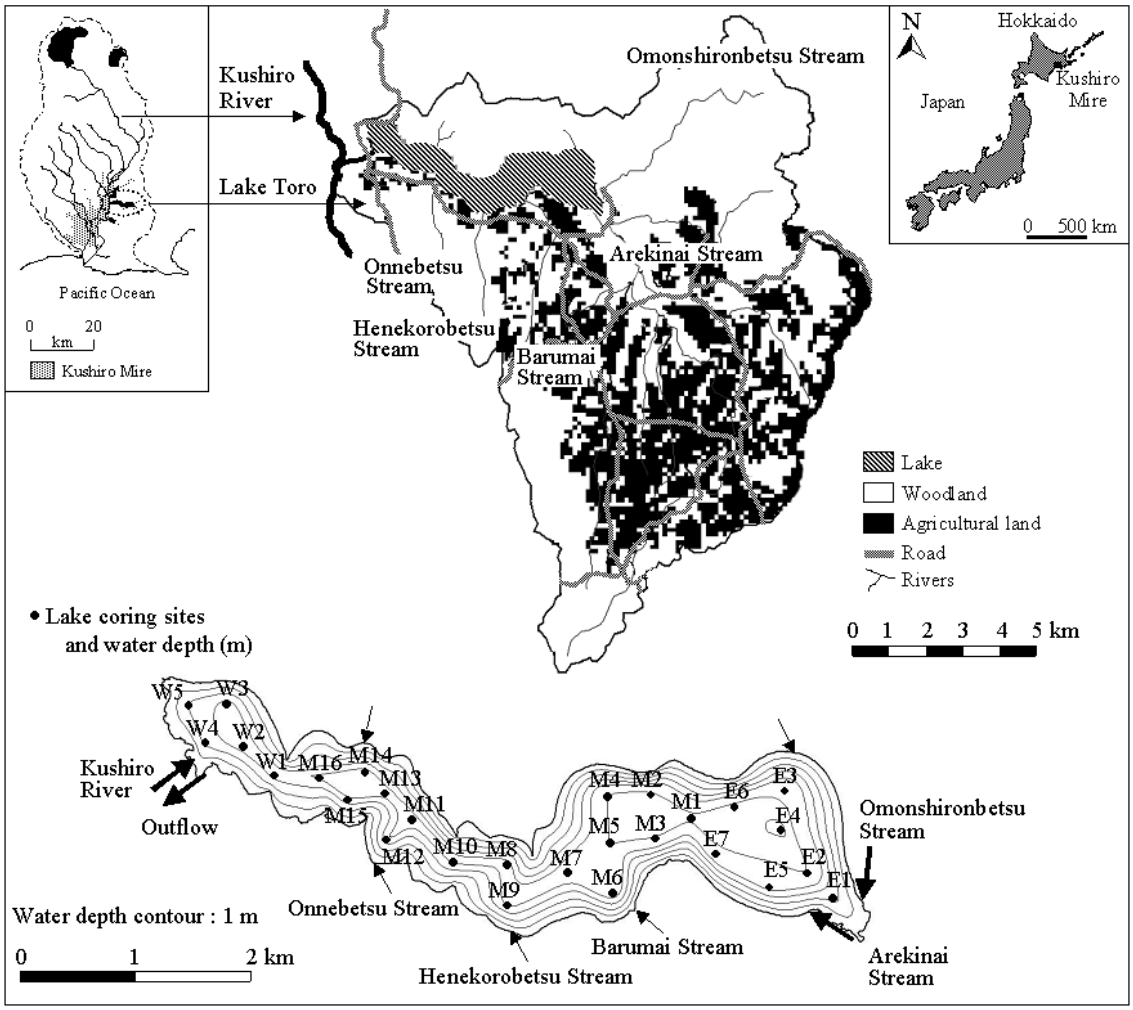
Kushiro River
Lake Toro
Pacific Ocean
0 20
km
Kushiro Mire
Omonshironbetsu Stream
Onnebetsu Stream
Henekorobetsu Stream
Barumai Stream
Arekinai Stream
N
Hokkaido
Japan
Kushiro Mire
0 500 km
Lake
Woodland
Agricultural land
Road
Rivers
0 1 2 3 4 5 km
• Lake coring sites and water depth (m)
W5 W3 W4 W2 W1 M16 M14 M13 M11 M15 M12 M10 M8 M9 M7 M6 M5 M4 M3 M2 M1 E6 E7 E5 E3 E4 E2 E1
Kushiro River
Outflow
Omonshironbetsu Stream
Water depth contour : 1 m
0 1 2 km
Onnebetsu Stream
Barumai Stream
Henekorobetsu Stream
Arekinai Stream

Figure 1

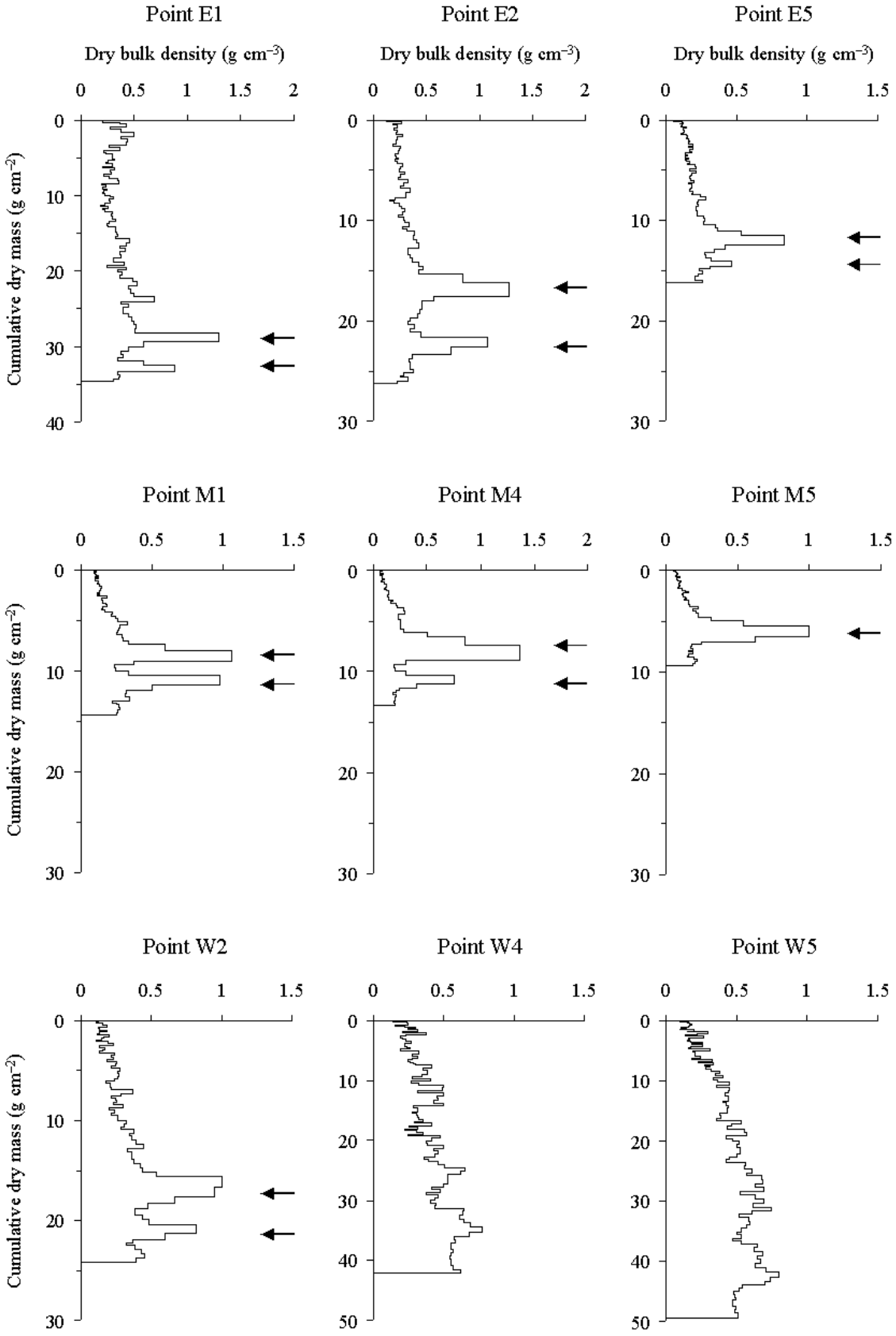
Point E1
Point E2
Point E5
Point M1
Point M4
Point M5
Point W2
Point W4
Point W5
Dry bulk density (g cm⁻³)
Cumulative dry mass (g cm⁻²)

Figure 2

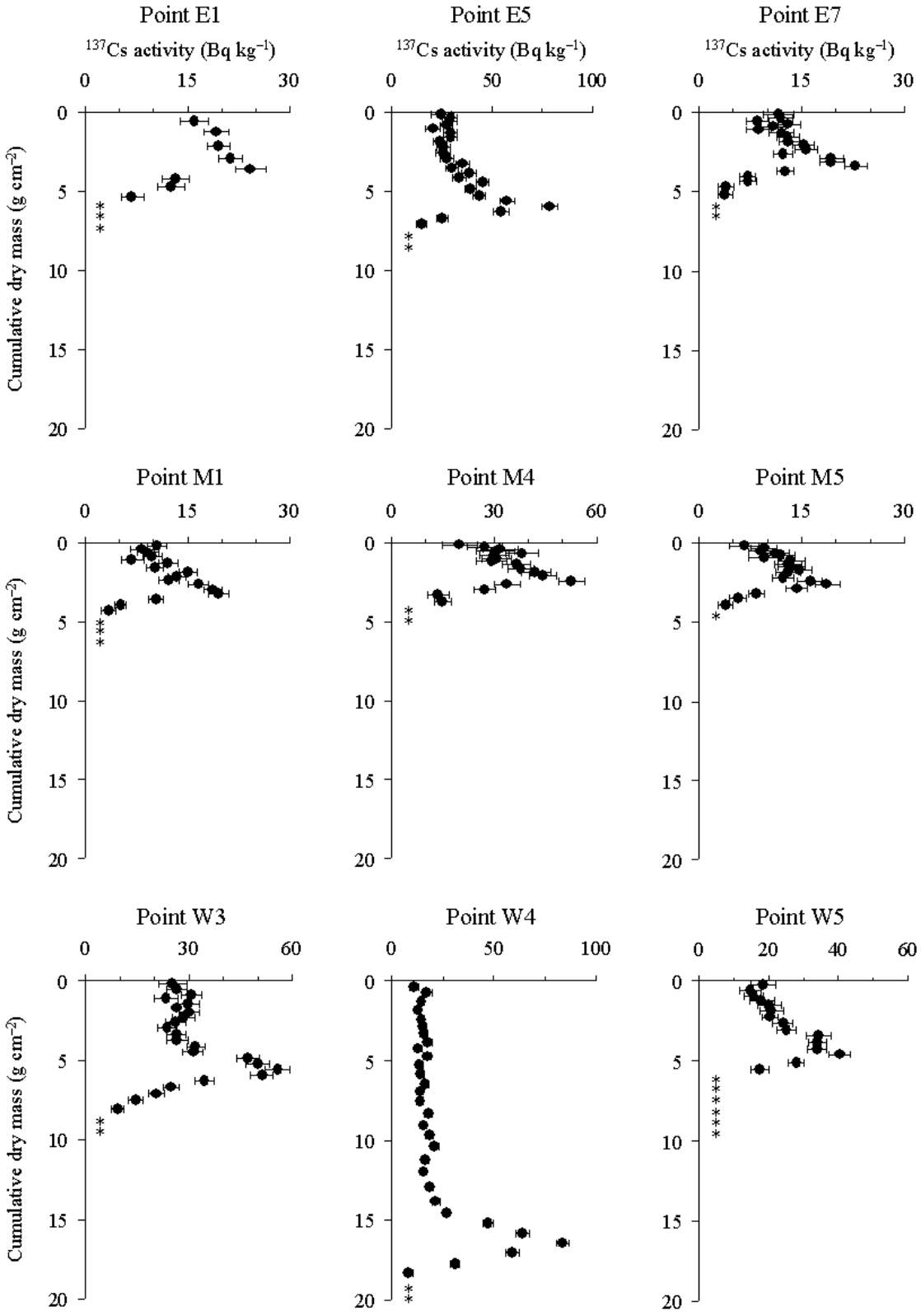
Point E1
Point E5
Point E7
Point M1
Point M4
Point M5
Point W3
Point W4
Point W5
137Cs activity (Bq kg−1)
Cumulative dry mass (g cm−2)

Figure 3

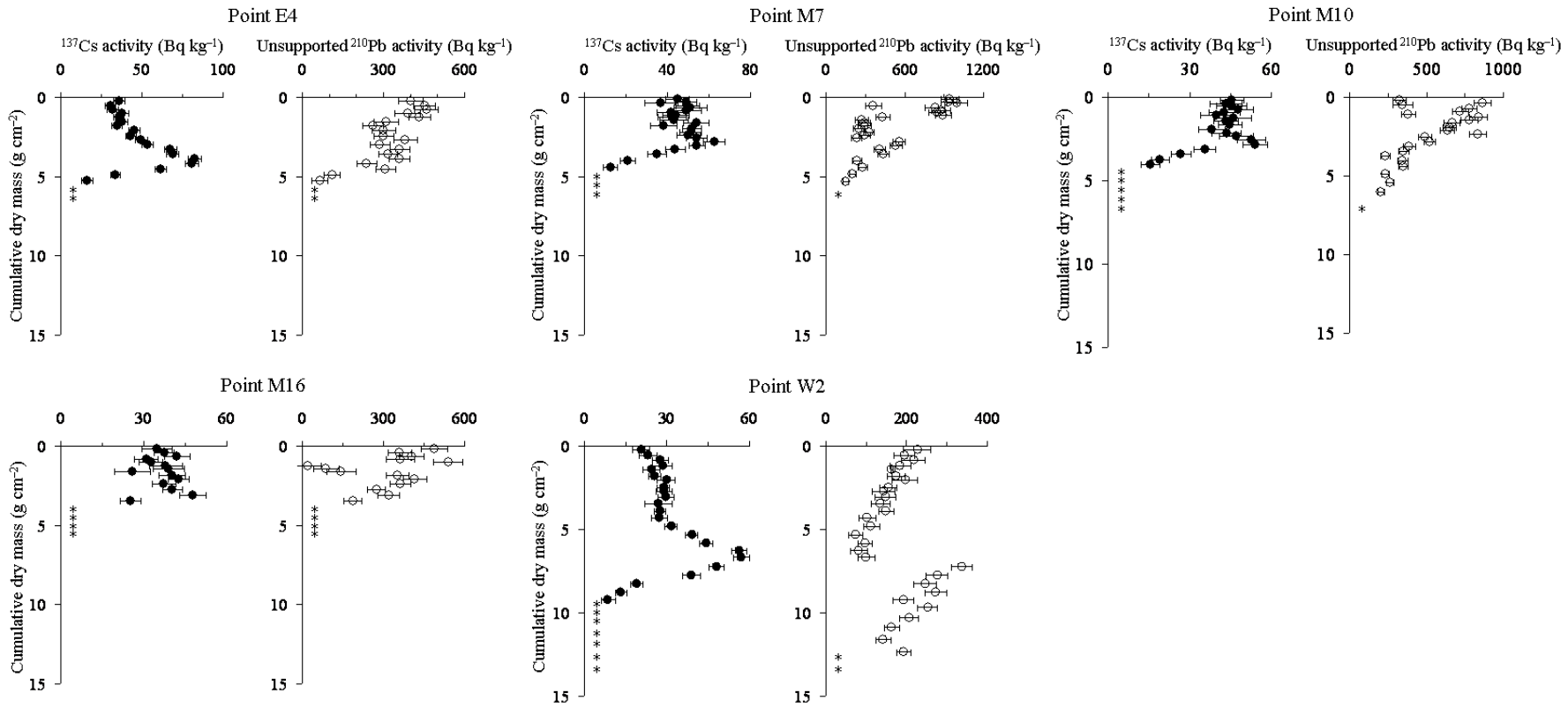
Point E4
Point M7
Point M10
Point M16
Point W2
137Cs activity (Bq kg−1)
Unsupported 210Pb activity (Bq kg−1)
Cumulative dry mass (g cm−2)

Figure 4

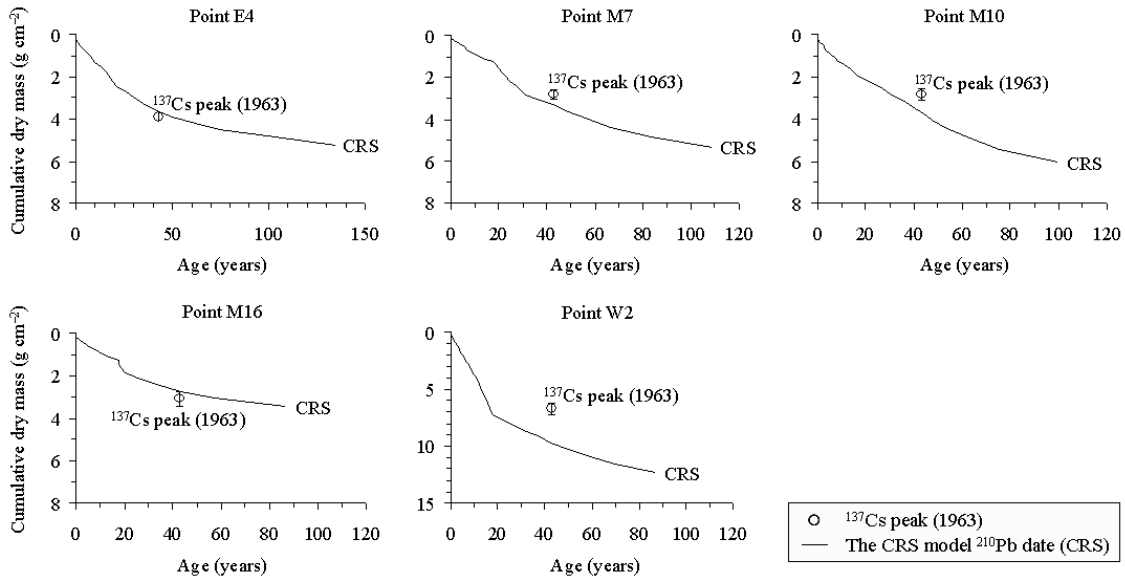
Point E4
Point M7
Point M10
Point M16
Point W2
Cumulative dry mass (g cm-2)
Age (years)
137Cs peak (1963)
CRS
137Cs peak (1963)
The CRS model 210Pb date (CRS)

Figure 5

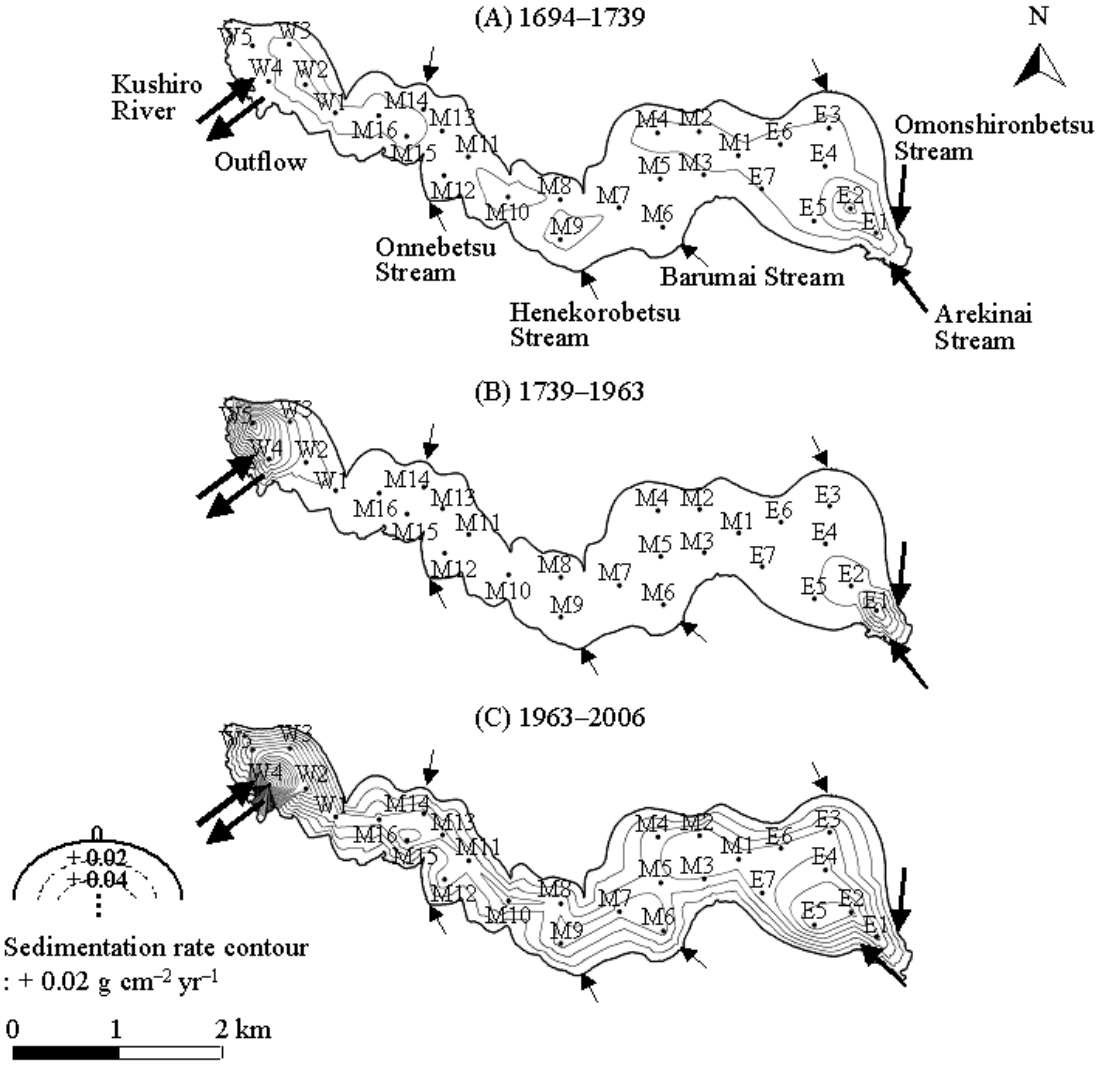
(A) 1694–1739
N
Kushiro River
Outflow
Omonshironbetsu Stream
Onnebetsu Stream
Henekorobetsu Stream
Barumai Stream
Arekinai Stream
(B) 1739–1963
(C) 1963–2006
0
+ 0.02
+ 0.04
Sedimentation rate contour
: + 0.02 g cm−2 yr−1
0 1 2 km

Figure 6

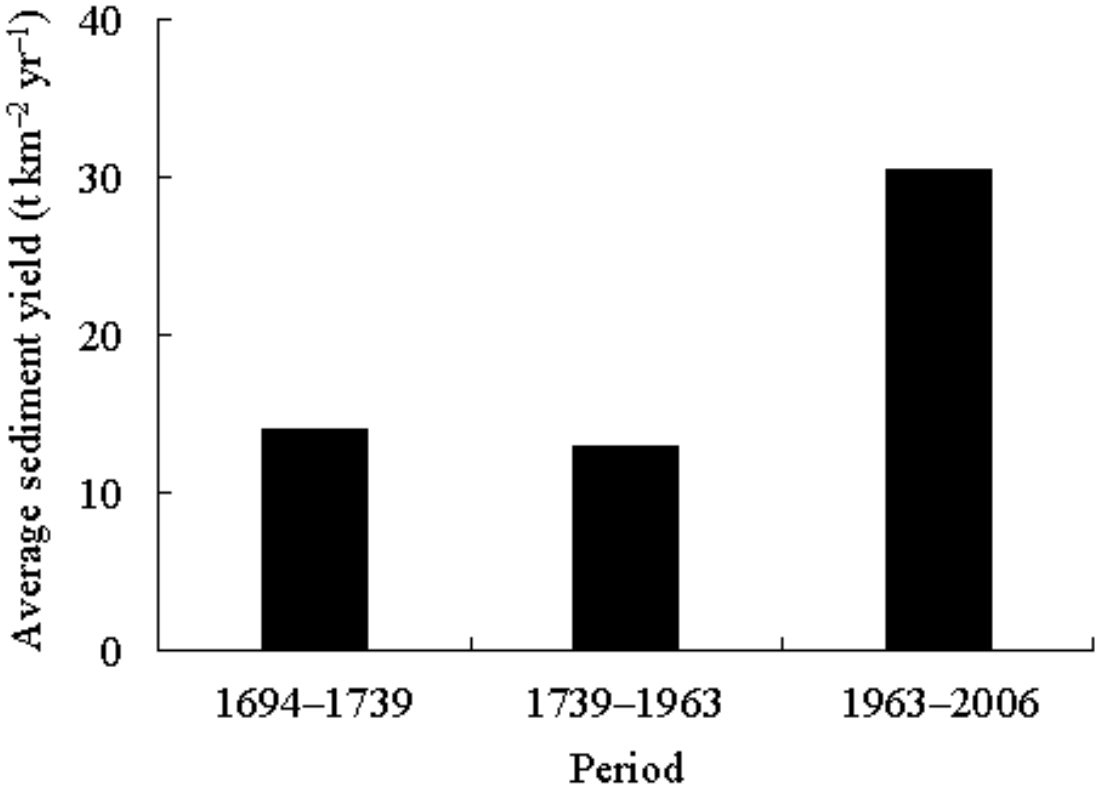
Average sediment yield (t km^{-2} yr^{-1})
40
30
20
10
0
1694–1739
1739–1963
1963–2006
Period

Figure 7